JACS
JOURNAL OF THE AMERICAN CHEMICAL SOCIETY
Article
pubs.acs.org/JACS

Identical Location Transmission Electron Microscopy Imaging of Site-Selective Pt Nanocatalysts: Electrochemical Activation and Surface Disordering

Rosa M. Arán-Ais,[†] Yingchao Yu,[‡] Robert Hovden,[§] Jose Solla-Gullón,[†] Enrique Herrero,[†] Juan M. Feliu,*[,†] and Héctor D. Abruña*[,‡]

[†]Instituto de Electroquímica, Universidad de Alicante. Apdo 99, 03080, Alicante, Spain

[‡]Department of Chemistry and Chemical Biology, Baker Laboratory and [§]School of Applied and Engineering Physics, Cornell University, Ithaca, New York 14853, United States

Supporting Information

ABSTRACT: We have employed identical location transmission electron microscopy (IL-TEM) to study changes in the shape and morphology of faceted Pt nanoparticles as a result of electrochemical cycling; a procedure typically employed for activating platinum surfaces. We find that the shape and morphology of the as-prepared hexagonal nanoparticles are rapidly degraded as a result of potential cycling up to +1.3 V. As few as 25 potential cycles are sufficient to cause significant degradation, and after about 500−1000 cycles the particles are dramatically degraded. We also see clear evidence of particle migration during potential cycling. These finding suggest that great care must be exercised in the use and study of shaped Pt nanoparticles (and related systems) as electrocatlysts, especially for the oxygen reduction reaction where high positive potentials are typically employed.

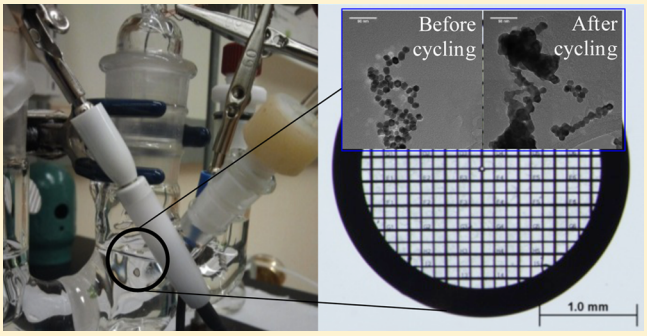

INTRODUCTION

The continued consumption of our natural, and increasingly scarce, resources makes necessary the use of alternative and renewable energy sources, such as wind and solar energy generation. Although fuel cells were initially conceived as attractive devices for the generation of electricity, (higher efficiencies and lower emissions) today the main applications for this technology are directed to portable or stationary electricity generation and power for transportation.[1−3] Nevertheless, the development and deployment of inexpensive, efficient, and reliable fuel cells is still very challenging, since several crucial issues must be resolved before their commercialization and deployment. The chemical reactions that produce the electrical current, and the nature of the electrodes where they take place, play key roles in the way fuel cells operate. In this context, many reactions of importance in electrocatalysis are known to be "structure sensitive", and surface structure effects in their electrocatalytic reactivity can be assessed through the use of single crystal electrodes. The information derived from such studies can be applied to the development of new and better performing catalysts for polymer electrolyte membrane fuel cells (PEMFC). Platinum (Pt) is still the most catalytic single metal for both oxygen reduction (ORR) and hydrogen oxidation (HOR) reactions in these devices, although it is possible to enhance the activity of Pt-based catalysts by modulating its size, morphology, and/or composition.[4−7]

Nanocrystals exhibit unique chemical and physical properties, determined both by the nature and the crystallographic structure of the surface atoms. In terms of the effects of morphology on electrocatalytic activity, numerous strategies have been developed over the past decades to obtain nanocrystals with preferential shape,[8−13] since the shape of a nanoparticle can be directly related to its surface structure.[4,14,15] In the vast majority of cases, it has been necessary to use stabilizing agents to mitigate aggregation and achieve the desired form. These stabilizing agents must be removed from the surface prior to electrochemical characterization, inasmuch as the understanding of heterogeneous chemical reactions (which includes electrochemical processes) requires clean surfaces. Since the flame-annealing treatment,[16] developed for obtaining clean and well-ordered bulk surfaces, cannot be applied to nanoparticles, a suitable cleaning procedure (specific for each synthesis method) must be developed/applied to remove the traces of materials employed in the synthesis from the nanocatalysts' surface without perturbing the nanosurface structure.[17]

Electrochemical activation has been the most widely used procedure, in the literature, to clean Pt nanoparticles prior to electrochemical experimentation.[18] The impurities on the

Received: September 10, 2015
Published: November 2, 2015

DOI: 10.1021/jacs.5b09553
J. Am. Chem. Soc. 2015, 137, 14992−14998

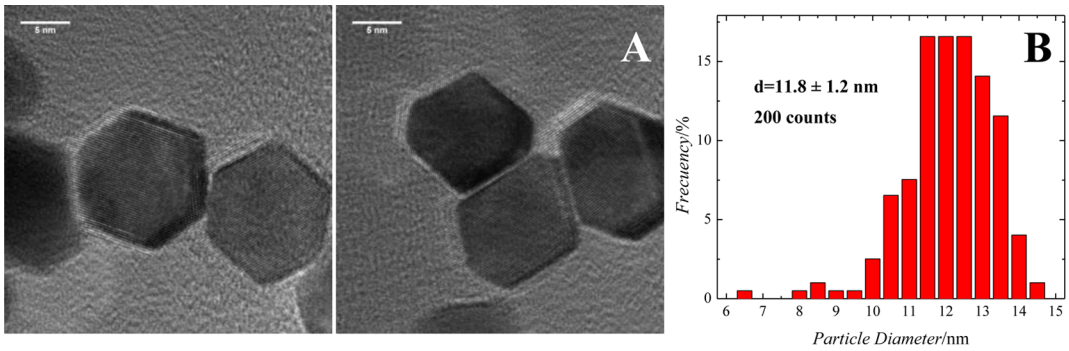

Figure 1. (A) HRTEM images of surfactant-free (as prepared) Pt NPs before cycling; faceting is clearly seen in the shaped particles. (B) Histogram of the NP diameter obtained from TEM images before cycling.

platinum surface are oxidatively desorbed at high positive potentials, leading to the activation of the electrode surface. Finally, a uniform and stable voltammetric profile is attained, independent of the initial state of the surface. However, some capping agents, like polyvinylpyrrolidone (PVP) or the mixture oleylamine/oleic acid (OLA/OA), are so strongly attached/adsorbed that they inhibit the electrochemical oxidation, rendering the potential cycling method ineffective.[17,19,20] Nevertheless, the oxidation of the surfaces and their subsequent reductions are known to be powerful tools to eliminate weakly bonded impurities, though increasing the surface disordering and thus the roughness of the surface of the nanoparticles.[21−24] Therefore, the classical electrochemical activation should not be applied when working with shaped-controlled nanoparticles since it significantly compromises the surface structure of the catalysts, leading to changes in activity.

Electrocatalyst degradation, in terms of changes in the surface structure and composition and loss of active area, can be monitored, *in situ*, by cyclic voltammetry. The modifications observed in the voltammetric profile after potential cycling have been widely studied, both with single crystal Pt electrodes[25,26] and shaped nanoparticles.[17] However, there are numerous publications[27−30] in which electrochemical activation is applied to achieve "clean" voltammetric profiles on shaped nanoparticles, disregarding the effects that this procedure may have on the catalyst's surface structure.[4,14,15]

In this study we report, using identical location transmission electron microscopy (IL-TEM) on the influence of the classical electrochemical activation (as described above) on the morphology of shaped Pt nanoparticles. This technique represents a powerful tool to study localized changes (in terms of size, shape, and agglomeration state)[31−36] produced on the nanocatalyst layer under the conditions in which the voltammetric study is performed. With the aim of investigating the structural changes of faceted Pt nanoparticles during an intensive electrochemical potential cycling, the nanoparticles were deposited onto a carbon coated gold TEM grid. This procedure allows for the correlation between the electrochemical response and the TEM analysis, unambiguously showing that potential cycling causes dramatic modifications to the surface structure and shape of the Pt nanoparticles, inducing particle coalescence and migration along the TEM grid.[37]

EXPERIMENTAL SECTION

Synthesis and Characterization of Pt Nanoparticles. Truncated octahedral Pt nanoparticles were synthesized by the method reported by Zhang et al.[38] and cleaned by the protocol described by Arán-Ais et al.[17] A dilute aqueous suspension of these Pt nanoparticles was sonicated, pipetted onto a labeled 2.5 mm diameter gold TEM grid (purchased from Electron Microscopy Sciences) coated with a thin carbon film, and allowed to dry overnight at room temperature. After the images of the as-prepared catalyst were taken, the TEM grid was punched with a fine gold wire and attached to a platinum holder in order to make the electrical contact. Accelerated durability testing was carried out by applying cyclic potential sweeps between +0.05 and +1.3 V at 50 mV/s in a 0.5 M H_2SO_4 solution at room temperature. A conventional three-electrode electrochemical cell was employed, using a platinum wire as the counter electrode and a reversible hydrogen electrode (RHE) as the reference electrode. Figure S1 shows the assembly for the electrochemical study. The supporting electrolyte was prepared from H_2SO_4 (Fisher Chemical) using ultrapure Millipore water (18.2 MΩ cm^{-1}). The electrode potential was controlled using a Solartron model 1280 B electrochemistry station.

A Tecnai F20 TEM operated at 200 kV was used for acquiring the TEM and high-resolution TEM (HRTEM) images. Scanning transmission electron microscopy (STEM) images and nanoarea electron diffraction patterns were acquired using the same equipment.

RESULTS AND DISCUSSION

Since the Pt nanoparticles used were deposited directly onto the thin carbon TEM grid, it was necessary to find a location on the TEM grid where no agglomeration was found, allowing for HRTEM imaging of individual nanoparticles. Figure S2 displays the TEM image of the location subjected to study. The high level of nanoparticle agglomeration in some regions points out the cleanliness of the sample, i.e., the effective removal of the stabilizing agents from the surface. The presence of such compounds tends to favor formation of nanoparticle arrays and superlattices[28,38−40] due to substrate−solvent interactions. Such a situation is clearly not desirable when trying to correlate the electrochemical response with the TEM images, since the incomplete removal of impurities from the synthesis would compromise electrochemical characterization.[17]

Figure 1A shows a HRTEM image of the as-prepared Pt nanoparticles which exhibit a hexagonal shape, corresponding to a (111)-(100) preferential orientation. These truncated-octahedral (TO) Pt nanoparticles were used with the aim of gaining insights into the effects of potential cycling on the different crystallographic orientations of the nanoparticles. Octahedrally and TO-shaped Pt nanoparticles provide beneficial morphologies with catalytically active sharp corners and edges. More than 200 particles from different parts of the grid were used to estimate the mean diameter (11.8 ± 1.2 nm) and size distribution of the nanoparticles (Figure 1B). The *d*-spacing for adjacent lattice fringes measured from several sites

DOI: 10.1021/jacs.5b09553
J. Am. Chem. Soc. 2015, 137, 14992−14998

was in good agreement with the {111} interplanar distance of the face-centered cubic (fcc) bulk Pt.[40−42]

Once the Pt nanoparticles were characterized by TEM, the carbon-coated TEM gold grid was transferred to an electrochemical cell (Figure S1A), where the cyclic voltammogram (CV) of the as-prepared sample was recorded. Figure 2A shows

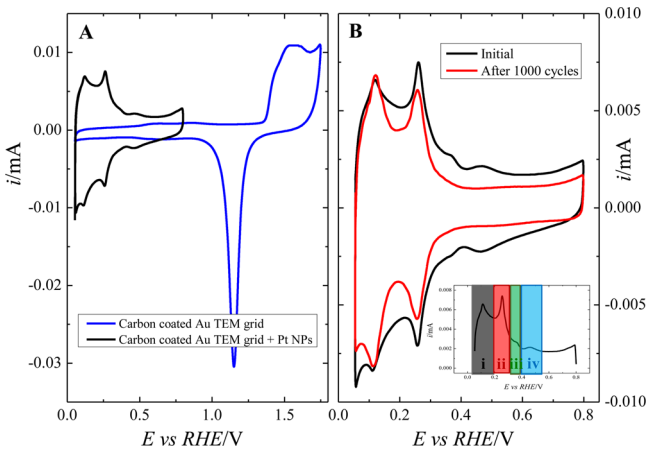

Figure 2. Voltammetric profiles in 0.5 M H_2SO_4 of the (A) carbon-coated Au TEM grid before (blue) and after (black) the addition of Pt shaped nanoparticles and (B) Pt shaped nanoparticles before and after 1000 potential cycles to +1.30 V. Sweep rate: 50 mV/s. The inset illustrates the different contributions (see text).

the CVs of the carbon-coated Au TEM grid, before and after adding the Pt NPs. The typical response of polycrystalline gold (blue trace) arises from the gold wire contact attached to the carbon coated Au TEM grid. Note that over the potential region of interest, the response of the carbon coated Au TEM grid does not affect the response from the Pt nanoparticles (black trace). As has been previously reported,[15] the voltammetric profile of Pt nanoparticles in a given supporting electrolyte can be used as a fingerprint of the different surface orientations. The specific adsorption of sulfate anions makes the hydrogen adsorption/desorption states better defined than those observed in perchloric acid solutions,[43] so the electrochemical activation (cycling) was performed in the former supporting electrolyte in order to clearly identify the changes that take place on the surface of the nanoparticle catalysts. As can be seen in Figure 2B, the initial voltammetric profile of the Pt nanoparticles (black trace) exhibited four characteristic features/regions: (i) a peak at +0.125 V, which is related to (110)-type sites; (ii) a peak at +0.27 V, which contains contributions from (100) steps sites on (111) terraces and the sites close to the steps on (100) terraces; (iii) signals at +0.35−0.37 V correlated to (100) bidimensional terraces; and (iv) signals at +0.5 V, attributed to the bidimensionally ordered (111) terraces. The inset illustrates the various contributions. As expected, the CV obtained is consistent with the shape of the nanoparticles observed in the TEM images. Subsequently, the working electrode (carbon-coated gold TEM grid plus Pt nanoparticles) was cycled 1000 times between +0.05 and +1.3 V at a sweep rate of 50 mV/s. The upper potential limit applied plays a key role as it determines the surface reconstructions. The choice of the upper limit was based on three reasons: (i) to completely perturb the well-ordered surface domains of the nanoparticles, (ii) reproduce the conditions used in the literature for performing electrochemical activation,[18,28] and (iii) simulate start-up/shutdown cycling tests in PEMFC.[44] The CV recorded after this treatment is shown in Figure 2B (red trace). As can be seen, the characteristic voltammetric profile of (111)-(100) preferentially oriented Pt nanoparticles evolves into the response typical of polyoriented/polycrystalline Pt nanoparticles. In addition, there is a clear loss of electrochemical surface area which was determined by integrating the area under the hydrogen adsorption/desorption region[15] (after subtraction of the double layer contribution) and which was calculated to be approximately 13% of the initial charge, which can be attributed to three main factors: (i) detachment of the NPs from the TEM grid, (ii) platinum dissolution, and/or (iii) coalescence of neighboring particles (agglomeration).

The characteristic (physical) shape of the group of NPs enabled the clear identification of their exact (identical) location before and after potential cycling allowing for a direct assessment of the effects of potential cycling on the Pt nanoparticles. Figure 3 shows the dramatic modifications to the

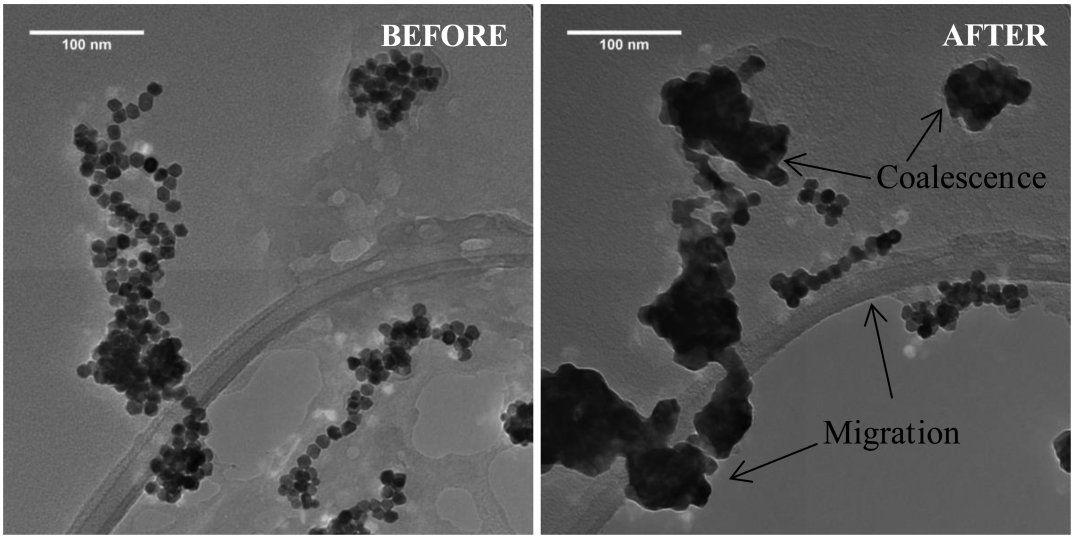

Figure 3. IL-TEM of the same location before and after 1000 cycles up to +1.3 V. Effects of coalescence and migration are clearly evident and indicated in the figure.

DOI: 10.1021/jacs.5b09553
J. Am. Chem. Soc. 2015, 137, 14992−14998

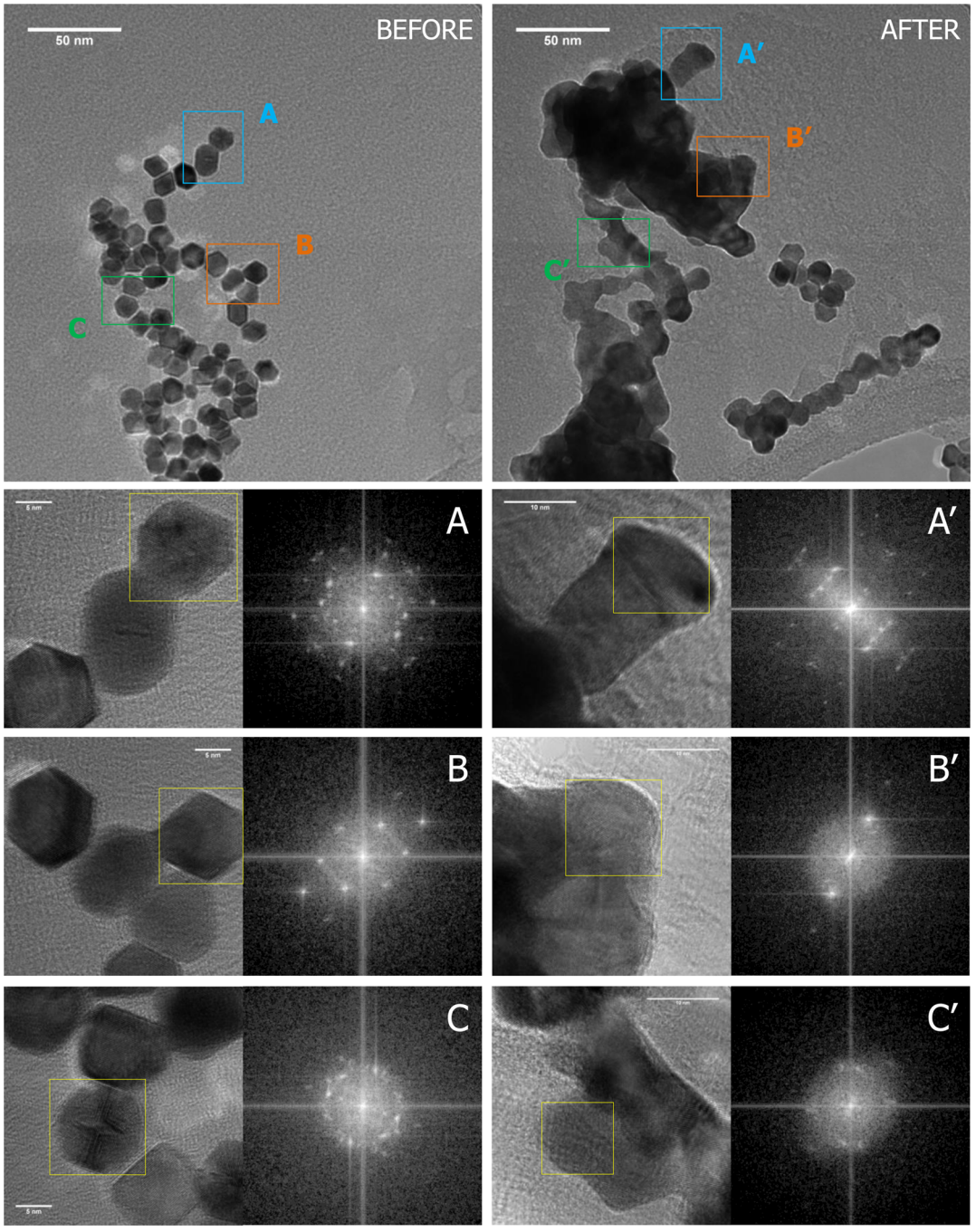

Figure 4. IL-TEM and IL-HRTEM images of the shaped Pt nanoparticles before (left side) and after (right side) 1000 potential cycles. FFT of the selected areas are shown next to each HRTEM image.

structure, shape, and distribution of the shaped nanoparticles after 1000 cycles, up to +1.30 V. The potential cycling has induced the coalescence of nanoparticles and their migration along the TEM grid. Some particle loss is also observed. Particle detachment and migration are interrelated, since both processes can be considered to be a consequence of the weakening of the interactions between the carbon film, on the TEM grid, and the Pt nanoparticles. The former process was expected to occur since it has already been observed for carbon-supported nanoparticles.[45] Movement and sintering of Pt nanoparticles have also been observed under ORR conditions.[46] Figure 3 shows that some fragments of NPs have also migrated along the TEM grid.

In addition to Pt dissolution/aggregation, the corrosion of the carbon support must also be taken into account. Degradation of the support, which can be seen in Figure 3, in turn, facilitated particle migration. Corrosion of the carbon support depends on the nature of the media (oxidizing, reducing, or neutral) and the upper potential limit used in accelerated stress tests.[47] It has also been found that the support can be corroded at temperatures close to the actual operating conditions of PEMFCs.[48]

Besides the effects of coalescence and migration, the most striking effect of the potential cycling is the strong surface modification of the Pt nanoparticles, which leads to the loss of their characteristic faceted structure. Consequently, the nano-

DOI: 10.1021/jacs.5b09553
J. Am. Chem. Soc. 2015, 137, 14992−14998

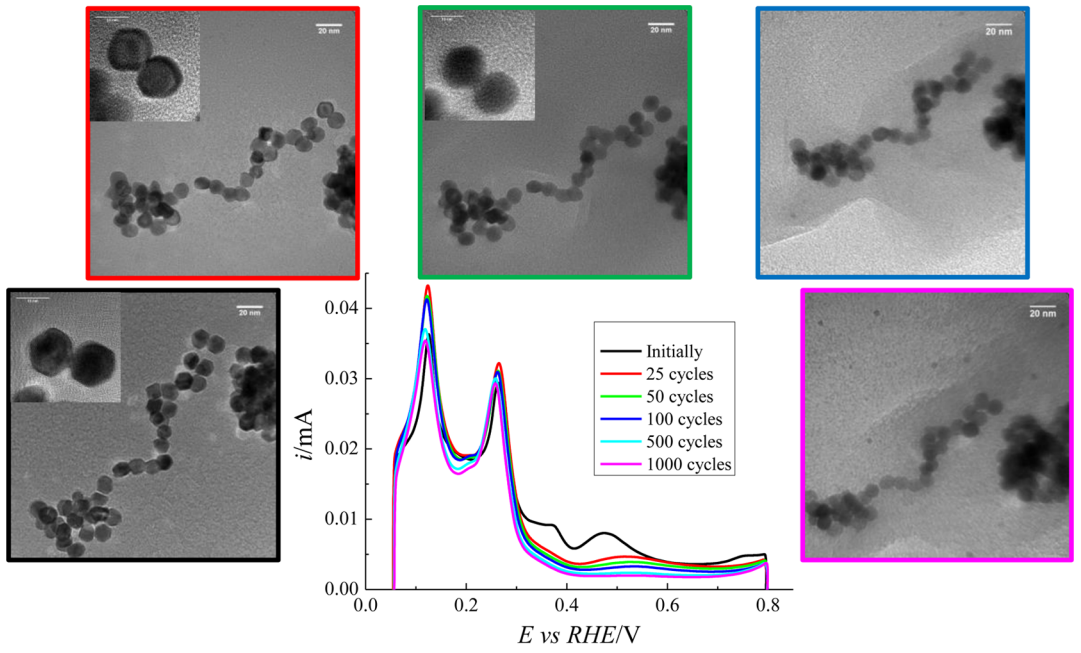

Figure 5. CVs in 0.5 M H_2SO_4 and IL-TEM images before and after 25, 50, 100, 500, and 1000 cycles up to 1.3 V, 50 mV/s. Colors indicate the correspondence between the voltammetric profiles and the TEM images. Insets show enlarged views of the indicated areas.

catalysts clearly lose their site-selective activity and ostensibly the purpose for which they were synthesized.

In order to gain a deeper understanding of the consequences of the potential cycling, specific particles were analyzed in more detail. Figure 4 presents HRTEM images of particles, as indicated, before and after electrochemical activation (1000 potential cycles). The coalescence of particles, loss of clearly defined faceted edges, and rounding of corners are dramatic. Fourier transforms (FFT) of the nanocrystals contain lattice peaks showing that some crystallinity is maintained within the particles after cycling, despite the structural reshaping and coalescence. This indicates that the presence of diffraction peaks can be misleading in assessing the effects of potential cycling on the Pt nanoparticles.

Since the effects on shaped Pt nanoparticles were quite dramatic after 1000 cycles of potential cycling between +0.05 and +1.3 V, the same catalyst was studied, both by TEM and electrochemically, after a smaller number of potential cycles, over the same potential window. Figure 5 shows the impact of potential cycling on a new deposit of the same sample of shaped Pt nanoparticles before and after 25, 50, 100, 500, and 1000 cycles. Note that after the 25th cycle, the loss of the features at +0.35−0.37 V and +0.5 V, related to the bidimensional domains of {100} and {111} symmetry, respectively, have disappeared. This result is of great importance since it confirms that using electrochemical activation with shaped nanocatalysts results in dramatic changes to their structure, in agreement with what had been previously demonstrated by cyclic voltammetry. Further electrochemical activation results in increasingly rounded shapes of the particles and a progressive increase of the contact area between the neighboring particles, due to coalescence processes. Similar results have been found for Pd cubic nanoparticles in alkaline media.[31]

The electrochemical active surface area (ECSA) was determined by integrating the charge involved in the so-called hydrogen UPD region, assuming 210 $\mu C/cm^2$ for the total charge after the subtraction of the double layer contribution. It was measured before and after 25 cycles and revealed an increase of 3.5%. This is likely due to an increase in surface roughness since the bidimensional domains evolve to steps and kinks sites. Surface reconstruction is more pronounced in nanoparticles than in single crystal electrodes since in the latter case, the presence of a bulk material provides more stability.[49] The voltammetric profiles after 25 cycles exhibited only small further changes, which indicates that most of the surface reconstruction has already taken place. However, there is a decrease in the measured ECSA, which can be related, again, to the coalescence of Pt nanoparticles. In this case, the loss of ECSA was calculated to be 11%, which is, within the experimental error, in agreement with the previous result obtained for the nanoparticles supported on the TEM grid.

It can be seen in Figure 5 that the TEM images become progressively "fuzzier" as the number of potential cycles is increased. The degrading effects that the electron beam can cause on Pt nanoparticles have been studied elsewhere,[50] where the presence of an oxidizing environment can lead to a decrease in the size of the Pt catalysts. The electron beam effects can be neglected since our TEM images were taken in high vacuum and the images were acquired in the shortest time possible. In order to verify that the identical location had not been damaged by the beam, some TEM images were taken in other regions of the TEM grid. The same "fuzziness" was observed in locations that were not exposed to the beam previously (figure S3), pointing out that the changes are from the electrochemical activation process and not from beam-induced damage.

■ CONCLUSIONS

We have studied the electrochemical potential cycling induced changes in the shape and morphology of (initially hexagonally) shaped Pt nanoparticles using IL-TEM. This potential cycling process, which is commonly employed for the activation of Pt surfaces, can give rise to dramatic changes in the shape and morphology of shaped Pt nanoparticles as well as to migration

DOI: 10.1021/jacs.5b09553
J. Am. Chem. Soc. 2015, 137, 14992−14998

of Pt nanoparticle clusters. We find that the shape and morphology of the as-prepared hexagonal nanoparticles are rapidly degraded as the function of potential cycling. As few as 25 potential cycles up to +1.3 V are sufficient to cause significant degradation, and after about 500−1000 cycles, the particles are dramatically altered. Given the recent emphasis on the use of shape-controlled nanoparticles for electrocatalysis, our findings suggest that great care must be exercised in the study of shaped Pt nanoparticles (and related systems) as electrocatlysts, especially for the ORR where high positive potentials are typically employed.

■ ASSOCIATED CONTENT

Supporting Information

The Supporting Information is available free of charge on the ACS Publications website at DOI: 10.1021/jacs.5b09553.

Images of electrochemical setup and the Au TEM grid used in the study; TEM images (PDF)

■ AUTHOR INFORMATION

Corresponding Authors

*hda1@cornell.edu

*juan.feliu@ua.es

Notes

The authors declare no competing financial interest.

■ ACKNOWLEDGMENTS

This work was carried out under financial support of MICINN (project no. CTQ2013-44083-P) and the energy materials center at Cornell (emc^2) an Energy Frontier Research Center funded by the U.S. Department of Energy, Office of Basic Energy Sciences, under award no. DESC0001086. R.M.A.-A. thanks the funding received from MICINN (EEBB-I-13-06184) to carry out a predoctoral stay in a foreign R&D center. This work and made use of TEM facilities of the Cornell Center of Materials Research, an National Science Foundation Materials Research Science and Engineering Center, under award no. DMR-1120296.

■ REFERENCES

(1) Wang, Y.; Chen, K. S.; Mishler, J.; Cho, S. C.; Adroher, X. C. *Appl. Energy* **2011**, *88*, 981.

(2) Kirubakaran, A.; Jain, S.; Nema, R. K. *Renewable Sustainable Energy Rev.* **2009**, *13*, 2430.

(3) Perry, M. L.; Fuller, T. F. *J. Electrochem. Soc.* **2002**, *149*, S59.

(4) Solla-Gullon, J.; Vidal-Iglesias, F. J.; Feliu, J. M. *Annu. Rep. Prog. Chem., Sect. C: Phys. Chem.* **2011**, *107*, 263.

(5) Bing, Y.; Liu, H.; Zhang, L.; Ghosh, D.; Zhang, J. *Chem. Soc. Rev.* **2010**, *39*, 2184.

(6) Gasteiger, H. A.; Markovic, N. M. *Science* **2009**, *324*, 48.

(7) Stamenkovic, V. R.; Fowler, B.; Mun, B. S.; Wang, G. F.; Ross, P. N.; Lucas, C. A.; Markovic, N. M. *Science* **2007**, *315*, 493.

(8) Guo, S.; Zhang, S.; Sun, S. *Angew. Chem., Int. Ed.* **2013**, *52*, 8526.

(9) Sau, T. K.; Rogach, A. L. *Adv. Mater. (Weinheim, Ger.)* **2010**, *22*, 1781.

(10) Xia, Y.; Xiong, Y.; Lim, B.; Skrabalak, S. E. *Angew. Chem., Int. Ed.* **2009**, *48*, 60.

(11) Tao, A. R.; Habas, S.; Yang, P. *Small* **2008**, *4*, 310.

(12) Burda, C.; Chen, X.; Narayanan, R.; El-Sayed, M. A. *Chem. Rev.* **2005**, *105*, 1025.

(13) Ahmadi, T. S.; Wang, Z. L.; Green, T. C.; Henglein, A.; El-Sayed, M. A. *Science* **1996**, *272*, 1924.

(14) Koper, M. T. M. *Nanoscale* **2011**, *3*, 2054.

(15) Vidal-Iglesias, F. J.; Aran-Ais, R. M.; Solla-Gullon, J.; Herrero, E.; Feliu, J. M. *ACS Catal.* **2012**, *2*, 901.

(16) Clavilier, J.; Armand, D.; Wu, B. L. *J. Electroanal. Chem. Interfacial Electrochem.* **1982**, *135*, 159.

(17) Aran-Ais, R. M.; Vidal-Iglesias, F. J.; Solla-Gullon, J.; Herrero, E.; Feliu, J. M. *Electroanalysis* **2015**, *27*, 945.

(18) Conway, B. E.; Angerstein-Kozlowska, H.; Sharp, W. B. A.; Criddle, E. E. *Anal. Chem.* **1973**, *45*, 1331.

(19) Yang, H.; Tang, Y.; Zou, S. *Electrochem. Commun.* **2014**, *38*, 134.

(20) Monzó, J.; Koper, M. T. M.; Rodriguez, P. *ChemPhysChem* **2012**, *13*, 709.

(21) Friedrich, K. A.; Henglein, F.; Stimming, U.; Unkauf, W. *Colloids Surf., A* **1998**, *134*, 193.

(22) Takasu, Y.; Ohashi, N.; Zhang, X. G.; Murakami, Y.; Minagawa, H.; Sato, S.; Yahikozawa, K. *Electrochim. Acta* **1996**, *41*, 2595.

(23) Takasu, Y.; Fujii, Y.; Yasuda, K.; Iwanaga, Y.; Matsuda, Y. *Electrochim. Acta* **1989**, *34*, 453.

(24) Clavilier, J.; Armand, D. *J. Electroanal. Chem. Interfacial Electrochem.* **1986**, *199*, 187.

(25) Bjorling, A.; Ahlberg, E.; Feliu, J. M. *Electrochem. Commun.* **2010**, *12*, 359.

(26) Björling, A.; Feliu, J. M. *J. Electroanal. Chem.* **2011**, *662*, 17.

(27) Kim, S.; Kim, C.; Lee, H. *Top. Catal.* **2010**, *53*, 686.

(28) Kang, Y.; Li, M.; Cai, Y.; Cargnello, M.; Diaz, R. E.; Gordon, T. R.; Wieder, N. L.; Adzic, R. R.; Gorte, R. J.; Stach, E. A.; Murray, C. B. *J. Am. Chem. Soc.* **2013**, *135*, 2741.

(29) Wu, J.; Gross, A.; Yang, H. *Nano Lett.* **2011**, *11*, 798.

(30) Zhong, C.; Liu, J.; Ni, Z.; Deng, Y.; Chen, B.; Hu, W. *Sci. China Mater.* **2014**, *57*, 13.

(31) Zadick, A.; Dubau, L.; Zalineeva, A.; Coutanceau, C.; Chatenet, M. *Electrochem. Commun.* **2014**, *48*, 1.

(32) Nikkuni, F. R.; Vion-Dury, B.; Dubau, L.; Maillard, F.; Ticianelli, E. A.; Chatenet, M. *Appl. Catal., B* **2014**, *156−157*, 301.

(33) Nikkuni, F.; Ticianelli, E.; Dubau, L.; Chatenet, M. *Electrocatalysis* **2013**, *4*, 104.

(34) Meier, J. C.; Katsounaros, I.; Galeano, C.; Bongard, H. J.; Topalov, A. A.; Kostka, A.; Karschin, A.; Schuth, F.; Mayrhofer, K. J. J. *Energy Environ. Sci.* **2012**, *5*, 9319.

(35) Zana, A.; Speder, J.; Roefzaad, M.; Altmann, L.; Bäumer, M.; Arenz, M. *J. Electrochem. Soc.* **2013**, *160*, F608.

(36) Mayrhofer, K. J. J.; Meier, J. C.; Ashton, S. J.; Wiberg, G. K. H.; Kraus, F.; Hanzlik, M.; Arenz, M. *Electrochem. Commun.* **2008**, *10*, 1144.

(37) Yu, Y.; Xin, H. L.; Hovden, R.; Wang, D.; Rus, E. D.; Mundy, J. A.; Muller, D. A.; Abruña, H. D. *Nano Lett.* **2012**, *12*, 4417.

(38) Kang, Y.; Pyo, J. B.; Ye, X.; Diaz, R. E.; Gordon, T. R.; Stach, E. A.; Murray, C. B. *ACS Nano* **2013**, *7*, 645.

(39) Kang, Y.; Ye, X.; Chen, J.; Cai, Y.; Diaz, R. E.; Adzic, R. R.; Stach, E. A.; Murray, C. B. *J. Am. Chem. Soc.* **2013**, *135*, 42.

(40) Wang, Z. L. *J. Phys. Chem. B* **2000**, *104*, 1153.

(41) Song, H.; Kim, F.; Connor, S.; Somorjai, G. A.; Yang, P. *J. Phys. Chem. B* **2005**, *109*, 188.

(42) Long, N. V.; Chien, N. D.; Hayakawa, T.; Hirata, H.; Lakshminarayana, G.; Nogami, M. *Nanotechnology* **2010**, *21*, 035605.

(43) Gómez, R.; Orts, J. M.; Feliu, J. M. In *ACS Symposium Series*; ACS: Washington, DC, 1997; Vol. *656*, p 156. 10.1021/bk-1997-0656.ch012

(44) Park, Y.-C.; Kakinuma, K.; Uchida, M.; Tryk, D. A.; Kamino, T.; Uchida, H.; Watanabe, M. *Electrochim. Acta* **2013**, *91*, 195.

(45) Solla-Gullón, J.; Lafuente, E.; Aldaz, A.; Martinez, M. T.; Feliu, J. M. *Electrochim. Acta* **2007**, *52*, 5582.

(46) Perez-Alonso, F. J.; Elkjær, C. F.; Shim, S. S.; Abrams, B. L.; Stephens, I. E. L.; Chorkendorff, I. *J. Power Sources* **2011**, *196*, 6085.

(47) Dubau, L.; Castanheira, L.; Berthomé, G.; Maillard, F. *Electrochim. Acta* **2013**, *110*, 273.

(48) Schlögl, K.; Mayrhofer, K. J. J.; Hanzlik, M.; Arenz, M. *J. Electroanal. Chem.* **2011**, *662*, 355.

(49) Vidal-Iglesias, F. J.; Solla-Gullón, J.; Herrero, E.; Montiel, V.; Aldaz, A.; Feliu, J. M. *Electrochem. Commun.* **2011**, *13*, 502.

DOI: 10.1021/jacs.5b09553
J. Am. Chem. Soc. 2015, 137, 14992−14998

(50) Simonsen, S. B.; Chorkendorff, I.; Dahl, S.; Skoglundh, M.; Sehested, J.; Helveg, S. *J. Am. Chem. Soc.* **2010**, *132*, 7968.

DOI: 10.1021/jacs.5b09553
J. Am. Chem. Soc. 2015, 137, 14992−14998